Insights into the contribution of Type VI Secretion towards AHPND pathogenesis

Damian Cavanagh[1, 2], Karina Martinez Lopez[1], Katie Sprinkel[1, 2], Brett Froelich[1]*

[1]Department of Biology, George Mason University, Manassas, Virginia, United States of America

[2]School of Systems Biology, George Mason University, Manassas, Virginia, United States of America

*Corresponding author

E-mail: bfroelic@gmu.edu (BAF)

Abstract

The Type VI Secretion System (T6SS) is a bacterial organelle that resembles a poison-tipped spear and is deployed by a wide range of Gram-negative species to intoxicate prokaryotic and eukaryotic prey. In this capacity, T6SSs are implicated in facilitating interbacterial antagonism and host-microbe interactions. Past reports have elucidated that many strains of *Vibrio parahaemolyticus* which cause Acute Hepatopancreatic Necrosis Disease (AHPND) in shrimp harbor two functional T6SSs (T6SS1 and T6SS2), leading to speculation about the contribution of these systems to disease progression. In the present study, we confirm the antibacterial functionality of T6SS1 and T6SS2 in the representative AHPND-causing *V. parahaemolyticus* (VP_{AHPND}) strain 13-306/D4. Employing a small-scale shrimp infection model, we then demonstrate that T6SS1 enhances the lethality of this isolate against whiteleg shrimp (*Litopenaeus vannamei*) postlarvae under warm, marine-like conditions. We additionally describe a novel antibacterial toxin/immunity pair encoded on pVA-like plasmids that features a putative colicin/bacteriocin effector domain. Our findings provide empirical evidence that Type VI Secretion (T6S) contributes to AHPND pathogenesis under conditions that are relevant to commercial aquaculture, inviting further studies to clarify the role of T6S as a virulence determinant.

Author summary

Type VI Secretion Systems (T6SSs) have drawn interest as versatile organelles that augment virulence and competitive fitness in myriad bacterial species. Included among these species are members of the genus *Vibrio*, many of which have clinical and commercial importance as pathogens or aquaculture pests. Isolates of *Vibrio parahaemolyticus* that harbor the $pirA^{vp}$ and $pirB^{vp}$ toxin genes encoded on pVA1-like plasmids have been identified as a causative agent of Acute Hepatopancreatic Necrosis Disease (AHPND), an illness that results in mass mortality events in shrimp aquaculture systems. It has been noted that, aside from $PirA/B^{vp}$, many VP_{AHPND} strains harbor two T6SSs (T6SS1 and T6SS2) which may be employed to outcompete and displace the native shrimp microbiome during colonization. In this study, we have directly assessed the effects of inactivating T6SS1 and T6SS2 on the lethality of a representative VP_{AHPND} isolate against whiteleg shrimp (*Litopenaeus vannamei*) postlarvae using an immersion challenge infection assay. Our findings indicate that T6SS1 contributes to the virulence of VP_{AHPND} against *L. vannamei* under warm, marine-like conditions, although further studies are needed to determine the underlying mechanisms. The present study helps to elucidate the factors involved in AHPND pathogenesis, thereby informing future efforts to develop countermeasures against this disease.

Introduction

Shrimp aquaculture constitutes one of the largest and fastest-growing sectors of food production throughout the world and serves as one of the major sources for high-protein seafood in South America, China, Thailand, Malaysia, and Vietnam. Given the scale of the shrimp aquaculture industry, production losses caused by infectious diseases such as Acute Hepatopancreatic Necrosis Disease (AHPND; formerly known as Early Mortality Syndrome or EMS) can prove economically devastating [1, 2]. Cumulative financial losses attributable to AHPND from the years 2010 to 2016 have been estimated at over $44 billion USD, and this figure likely constitutes a fraction of global losses that have occurred to date [2]. Further, mass mortality events caused by AHPND can significantly compromise the

socio-economic well-being of communities that lean heavily upon shrimp aquaculture for income and food production [2].

Past studies have identified *Vibrio parahaemolyticus* strains harbouring the plasmid-borne *pirA*^{vp}/*pirB*^{vp} toxin genes as the primary cause of AHPND, although isolates of related species such as *Vibrio campbellii* and *Vibrio owensii* have also been confirmed as etiologic agents [1, 3]. The substantial economic harm caused by AHPND-associated *V. parahaemolyticus* (VP_{AHPND}) has prompted numerous investigations to elucidate the mechanisms involved in pathogenesis. While the *pirA*^{vp} and *pirB*^{vp} genes encoded on pVA1-like plasmids have been cited as the main virulence genes responsible for necrosis of the shrimp hepatopancreas, it is speculated that other genomic elements are necessary for colonization and pathogenesis within the shrimp host [4, 5]. In particular, Type VI Secretion (T6S) has been consistently identified as a potential virulence determinant which may enable AHPND pathogenesis [5–7].

The Type VI Secretion System (T6SS) is a spear-like, membrane-anchored contractile injection system that shares evolutionary history with phage tail-associated protein complexes [8–10]. The T6SS apparatus consists of a central tube of stacking Hemolysin-coregulated protein (Hcp) monomers that terminate in a Valine-glycine repeat protein G (VgrG) spike. The VgrG spike protein, in turn, is adorned by a Proline-Alanine-Alanine-aRginine (PAAR) domain-containing protein that serves to sharpen the tip of the “spear” for more effective puncturing. The central tube of the T6SS is encompassed by an outer sheath which is anchored to the cell envelope by a baseplate complex [10]. Assembly, firing, and disassembly of the T6SS organelle is an energetically expensive process, and is often governed by complex regulatory networks [11, 12].

Effector toxins can be loaded onto the T6SS platform by several means, and are delivered into prey cells through an injection mechanism facilitated by contraction of the tail tube/sheath complex (**Fig 1**) [9]. A diverse arsenal of effector toxins and other T6SS cargo molecules have been described to date [13–15]. Although most effectors identified thus far are thought to be either specifically antibacterial or anti-eukaryotic, others exhibit mechanisms that allow them to function as trans-kingdom effectors. Some antibacterial effectors, such as those harboring a DNase or RNase domain, exert toxicity through nuclease activity, while others disrupt the prokaryotic cell envelope through pore formation, lipase activity, or damage to the cell wall [16, 17]. Effectors that intoxicate through more complex mechanisms have also been discovered. The *Pseudomonas aeruginosa* effector Tas1, for example, was shown to cause metabolic dysregulation and depletion of ATP in prey cells by rapidly synthesizing (p)ppApp [18]. Importantly, antibacterial effector genes are typically encoded beside a cognate immunity gene that mitigates self-intoxication and kin-killing by expressing an “antidote” protein that neutralizes effector toxicity [9, 13].

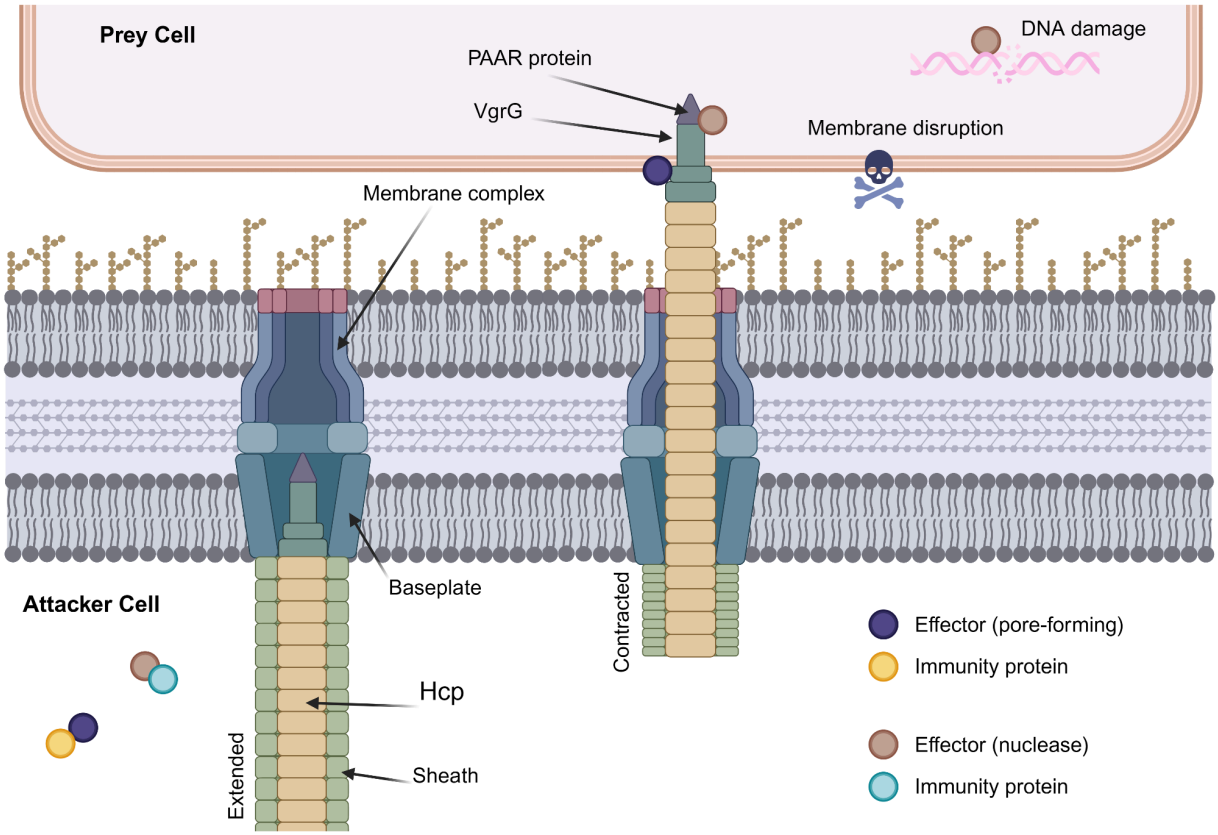

Fig 1. Structure and mechanism of the Type VI Secretion System (T6SS). The T6SS apparatus consists of a spiked tube which is surrounded by an outer sheath and anchored to the Gram-negative cell envelope by the baseplate complex. Contraction (firing) of the device allows for translocation of multiple effectors with distinct mechanisms into an adjacent cell. Image made with BioRender.

Type VI Secretion (T6S) has been implicated as a factor in the competitive fitness and virulence of a wide range of bacterial taxa, many of which belong to clinically significant genera such as *Yersinia*, *Pseudomonas*, and *Vibrio* [15, 19–22]. Some species that utilize T6S harbor more than one functional T6SS, each of which may be regulated independently and employed in different scenarios [23–25]. Further, species possessing more than one T6SS may deliver a different payload of protein effectors with each [15, 23]. It has been demonstrated that some T6SSs are used primarily to inject antibacterial effectors to antagonize non-kin bacterial competitors, while others facilitate virulence against eukaryotic targets such as host macrophages and other immune cells [9, 19].

Prior reports note that, in addition to the canonical T6SS2 found in nearly all strains of *V. parahaemolyticus*, many AHPND-associated isolates also harbor a conserved T6SS1, leading to conjectures about the role of these systems, and particularly T6SS1, in AHPND pathogenesis [5, 6]. Past studies of T6S in *V. parahaemolyticus* have demonstrated the antibacterial functions of T6SS1 and T6SS2, and progress has been made in elucidating the regulatory networks to which these systems are subject [23, 24, 26]. Within this framework, it has been speculated that one or both of these T6SSs confer a fitness advantage that allows VP_{AHPND} to overcome and displace the native shrimp microbiota, thereby facilitating colonization of the host [5, 6].

In addition to enabling interbacterial antagonism, T6SS1 and T6SS2 may also play a role in adhesion to host cells by *V. parahaemolyticus* [27–29]. Yu et al. (2012) demonstrate that inactivation of T6SS1 or T6SS2 via deletion of the corresponding *icmF* or *hcp* genes causes a defect in adhesion to cultured cell monolayers [27]. Notably, deletion of *icmF1* or *hcp1* was shown to reduce adhesion to monolayers of Caco-2 intestinal epithelial cells in addition to HeLa cell monolayers. In a separate study, Pinkerton et al. (2019) report defects in adherence to and invasion of CHSE-214 cells (Chinook salmon) by VP_{AHPND} isolates 13-306/D4 and 13-028/A3 following exposure to the natural antimicrobial mixture Auranta 3009 (A3009) [29]. Pinkerton et al. (2019) correlate these adhesion defects with downregulation of *hcp1* and *hcp2* as caused by A3009, and further show that administration of A3009 curtails post-infection mortality of *L. vannamei* challenged with VP_{AHPND} in a dose-dependent manner [29].

Although prior works either suggest or provide supporting evidence that T6S contributes to AHPND pathogenesis, direct investigations of T6SS1 and T6SS2 as virulence determinants are lacking. In this study, we empirically assess the extent to which these systems impact post-infection mortality in whiteleg shrimp challenged with the representative VP_{AHPND} strain 13-306/D4 or derived mutants.

Results

T6SS1 and T6SS2 mediate antibacterial activity in *V. parahaemolyticus* 13-306/D4

To begin our investigation, we identified *V. parahaemolyticus* 13-306/D4 (also listed as 13-306D/4, and abbreviated D4) as a suitable VP_{AHPND} strain for future experiments. This strain was originally isolated from the hepatopancreas of a Mexican shrimp specimen afflicted with AHPND, and has been shown to cause high levels of mortality in commercially-relevant species such as *L. vannamei* [30]. Additionally, D4 harbors a functional T6SS1 and T6SS2, both of which are expressed under appropriate conditions [6]. Notably, early reports of *in vitro* experiments suggest that T6SS1 is most active under warm, marine-like conditions (30°C, 3% [wt/vol] NaCl), while T6SS2 is primarily expressed at lower temperatures and salinities (23°C, 1% [wt/vol] NaCl) [6]. However, it has subsequently been shown that some strains of *V. parahaemolyticus* also exhibit T6SS2-mediated antibacterial activity under the warm, marine-like conditions that induce T6SS1 [25].

We first sought to evaluate how inactivation of T6SS1, T6SS2, or both systems would influence interbacterial killing by D4. To this end, we employed allelic exchange mutagenesis to delete the genes encoding Hcp1 and Hcp2 in D4, thus rendering one or both systems inoperable. The resulting D4 Δ*hcp1*, Δ*hcp2*, and Δ*hcp1/2* strains were subsequently used as attackers in a T6SS competition assay to compare the killing efficiency of T6SS-deficient mutants relative to the wild type D4 (**Fig 2A** and **Dataset S1**). Growth experiments were also performed to ensure that the above mutations did not incur a growth defect (**Fig 2B** and **Dataset S2**).

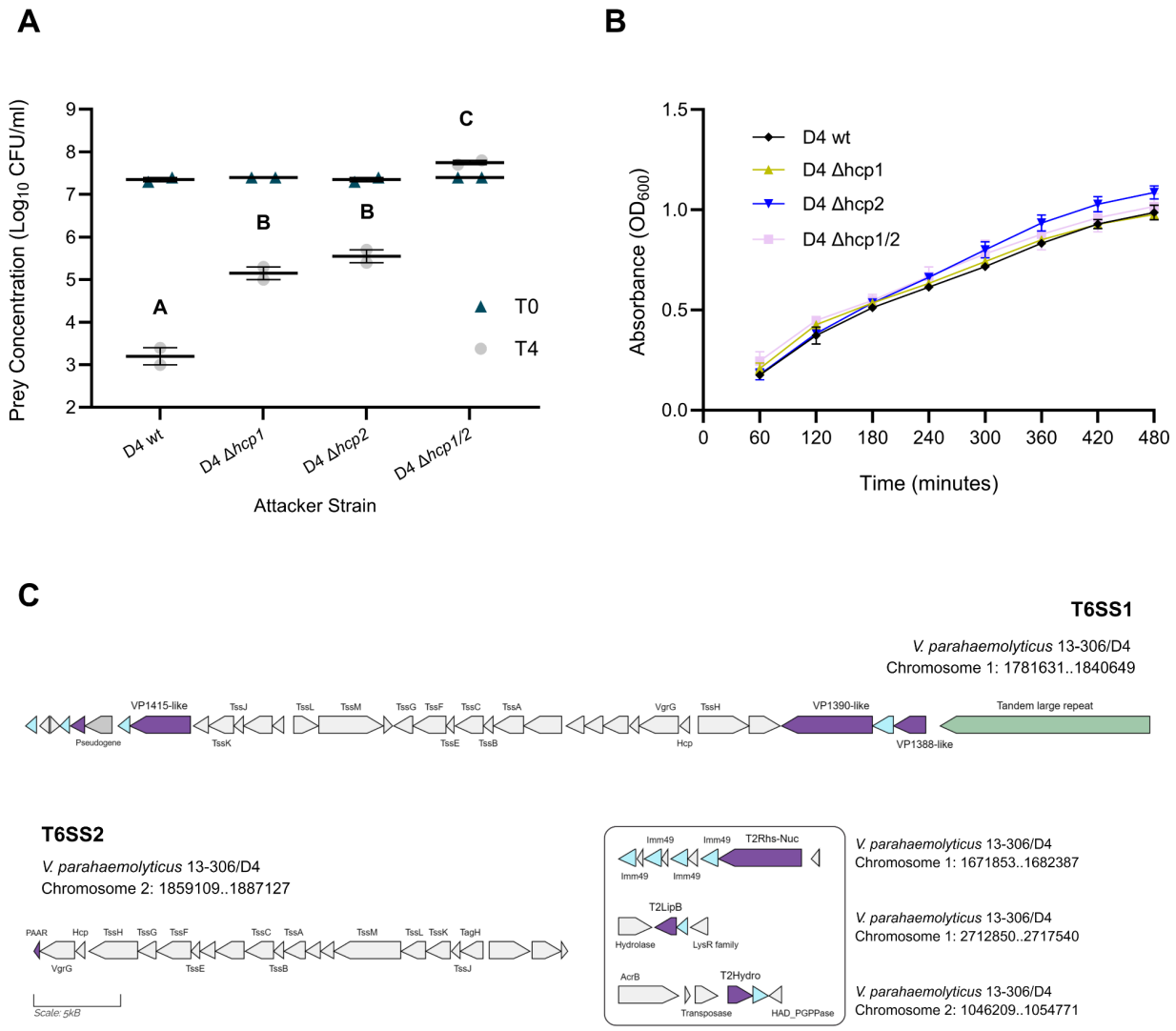

Fig 2. Comparison of *V. parahaemolyticus* 13-306/D4 parent and T6SS knockout strains. (A) Concentration of *E. coli* DH5α prey before (T_0, triangles) and after (T_4, circles) 4 hour co-incubation with the indicated *V. parahaemolyticus* attacker strain on Marine Luria Bertani at 30°C. Bars show mean ± SEM. T0 values are not statistically different ($p > 0.05$). T4 values with different letters are significantly different from each other ($p < 0.0001$). Data were analyzed using two-way ANOVA with Šídák's test for multiple comparisons. **(B)** Growth over time of *V. parahaemolyticus* 13-306/D4 and derived mutants, measured by absorbance (OD_{600}). Error bars represent SEM. Data in A and B represent two independent experiments with three technical replicates each. **(C)** T6SS core and accessory gene clusters in *V. parahaemolyticus* 13-306/D4. Features are colored to indicate functional categories. Genes coding for putative effector toxins (purple), putative immunity proteins (cyan), core T6SS structural components (light gray), and a TasL homolog (green) are indicated. Image made with Gene Graphics [31].

Wild type D4 demonstrated efficient killing of *E. coli* prey under warm, marine-like conditions on a solid surface (i.e., agar media containing 3% [wt/vol] NaCl, with a 4 hour incubation at 30°C). Deletion of either *hcp1* or *hcp2* alone attenuated but did not abolish ($p < 0.0001$) antibacterial activity, whereas deletion of both genes resulted in the inability to reduce prey CFU over the course of the assay ($p <$

0.0001). Remarkably, the individual contributions of T6SS1 and T6SS2 to antibacterial activity were similar (p = 0.17), indicating that D4 likely utilizes both systems for competition in warm, marine-like environments.

Our next aim was to characterize the repertoire of T6SS effector/immunity (E/I) pairs employed by D4. We began with a search for homologs of experimentally confirmed effectors reported in the literature, the results of which are depicted in **Fig 2C** and summarized in **Table 1**.

D4 CDS Region[#]	Product	Predicted Function	Known Effector/Cargo	Accession	Alignment Summary[&]	Source
Chr 1: 1821293–1826071 (-)	WP_085609853.1	VP1390-like effector	VP1390	BAC59653.1	99% QC; 26.93% ID	[33]
Chr 1: 1827178–1828872 (-)	WP_024699427.1	VP1388-like co-effector	VP1388	BAC59651.1	97% QC; 65.36% ID	[33]
Chr 1: 1787105–1790296 (-)	WP_031852689.1	PAAR-like and AHH domain protein	VP1415	BAC59678.1	63% QC; 50% ID	[32]
Chr 1: 1677092–1681462 (-)	WP_191786262.1	Rhs repeat and nuclease domain protein	T2Rhs-Nuc^{BB22OP}	WP_015296737.1	100% QC; 95.19% ID	[25]
Chr 1: 2714750–2715886 (-)	WP_020840162.1	Lipase	T2LipB^{BB22OP}	WP_015296300.1	100% QC; 99.47% ID	[25]
Chr 2: 1051957–1053264 (+)	WP_021451965.1	α/β hydrolase	T2Hydro^{RIMD}	BAC61690.1	100% QC; 100% ID	[25]

Table 1. Predicted T6SS effector and cargo proteins in *V. parahaemolyticus* 13-306/D4. Predicted effector and cargo molecules associated with T6SS1 and T6SS2 are shaded in yellow and blue, respectively. For blastp alignment results, see **Dataset S3**.

Genomic coordinates provided are in reference to the completed V. parahaemolyticus 13-306/D4 assembly, submitted to NCBI with accession SUB15344673. Chr, chromosome; (-/+), strand.

& Alignments were performed using the NCBI blastp suite on default parameters. D4 protein sequences were used as queries against reference protein sequences. QC, query coverage; ID, identity.

Inspection of the D4 genome revealed several gene products that putatively serve as effector toxins for delivery via T6S (**Dataset S3**). Included among these is a VP1415 homolog encoded a short distance downstream of *dotU* at one end of the T6SS1 core gene cluster. As with VP1415, the D4-encoded WP_031852689.1 harbors a PAAR-like domain and a C-terminal AHH nuclease motif [6, 32]. Located near the opposite end of the T6SS1 cluster is a tricistronic operon, the products of which putatively constitute a VP1388-1390-like effector module [33]. This operon is followed by a gene coding for a large tandem repeat protein (WP_318301207.1) with homology (34.04% identity, 99% query coverage, E-value 0.00) to the putative lipoprotein TasL (WP_135354012.1) from the bobtail squid symbiont *Aliivibrio fischeri* [34]. While not strictly a T6SS effector or cargo molecule, TasL is employed by *A. fischeri* to aggregate competitor cells within the host environment, thereby facilitating the close contact requisite for T6SS-dependent killing [34]. Among the T6SS2 effectors identified are a T2Rhs-Nuc ortholog with a Polymorphic Nuclease (PoNe) family C-terminal domain, and a homolog of the T2Hydro effector, both described by Salomon et al. (2022) [25]. D4 also encodes a homolog of T2LipB, which serves as a T6SS2 substrate but remains unconfirmed as an effector [25].

The AHPND-associated pVA plasmid harbors an effector with a predicted colicin domain as part of a toxin/immunity pair

Unexpectedly, our survey of the effector landscape in D4 revealed two pVA-encoded hypothetical proteins (WP_025789713.1 and WP_025789712.1) as a candidate E/I pair (**Figs 3A** and **3B**). A 4-bp overlap between the corresponding genes signified that WP_025789713.1 and WP_025789712.1 may be co-translated, as is often the case for antibacterial toxin/immunity pairs. Gene pairs coding for identical

proteins are likewise arranged on the pVA plasmids of geographically diverse VP_{AHPND} isolates including PSU5579 (Thailand), L2181 (Ecuador), and PH1339 (Philippines), and can also be found on homologous plasmids belonging to AHPND-causing *V. campbellii* and *V. owensii* strains [1, 3, 35]. While WP_025789713.1 is in some cases annotated as "SSU ribosomal protein S2p (SAe)", we suspect this is an error from the original RAST annotation of the pVA1 plasmid in 3HP [1]. While no domains are currently shown for WP_025789713.1 in the NCBI CDD, structure prediction using HHPred indicates a putative C-terminal colicin/bacteriocin domain and transmembrane helices.

Searching the literature for similar proteins revealed that WP_025789713.1 exhibits modest homology to previously reported T6SS effectors, including the predicted *Pantoea* effector ADU69816.1 (21.99% identity, 57% query coverage, E-value 4.0E-13) and the *V. coralliilyticus* effector XCY83140.1 (33.15% identity, 74% query coverage, E-value 5.0E-49) [36, 37]. Further queries against the NCBI nonredundant protein database yielded stronger matches to the PAAR domain protein HHC7385846.1 (51.54% identity, 89% query coverage, E-value 5.00E-136) from *V. parahaemolyticus* VB18PR-0247-2, and the *A. fischeri* protein OED55992.1 (61.10% identity, 73% query coverage, E-value 1.0E-138), which is encoded within a gene cluster that also codes for an Hcp, VgrG, and DUF4123 loading adapter protein (**Dataset S3**). Finally, WP_025789713.1 shares robust homology to the predicted T6SS RIX motif effector WP_130243383.1 (56.14% percent identity, 75% query coverage, E-value 2.0E-135), but does not appear to contain an N-terminal RIX motif itself [38].

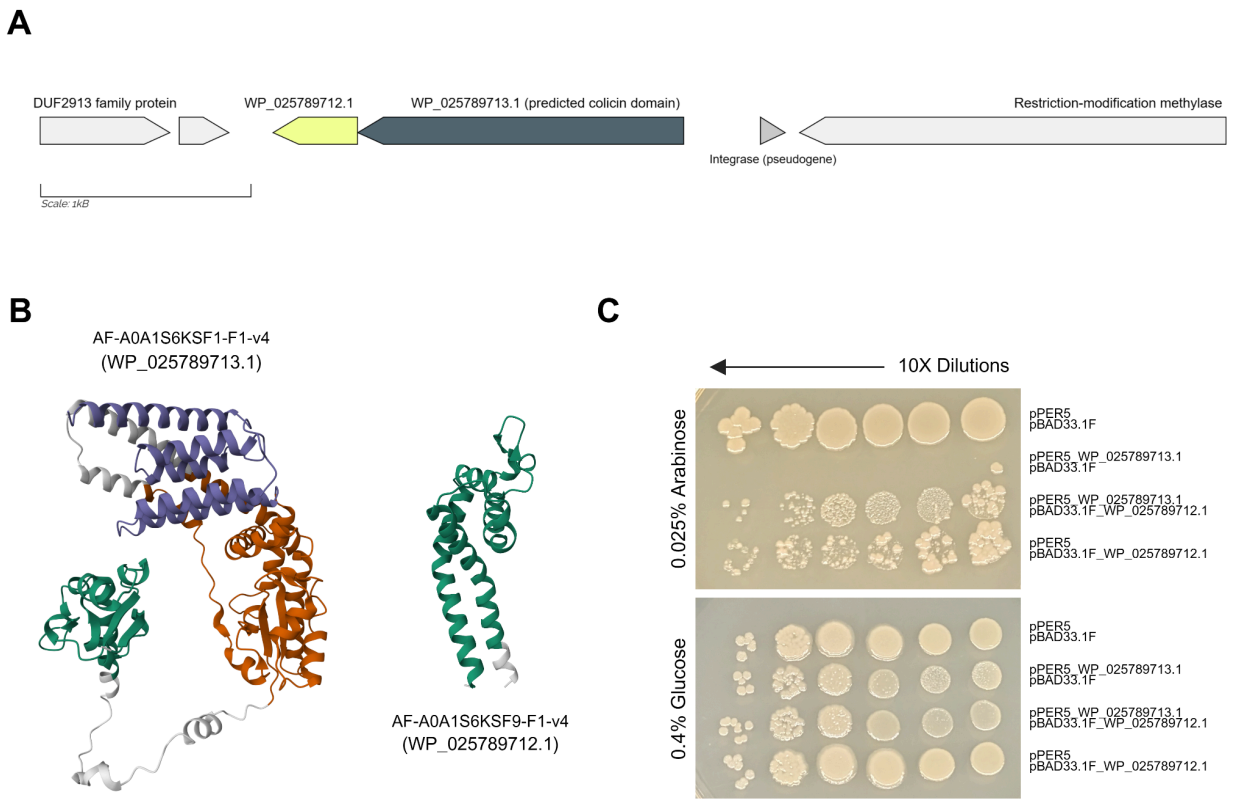

Fig 3. Analysis of WP_025789713.1 and WP_025789712.1 as an effector/immunity pair. (A) Genomic context of the bicistronic operon coding for WP_025789713.1 (lead gray) and WP_025789712.1 (yellow) on pVA1-like plasmids. Image made with Gene Graphics [31]. **(B)** AlphaFold structures of A0A1S6KSF1 (WP_025789713.1) and A0A1S6KSF9 (WP_025789712.1) from *V. owensii* SH14 [39]. Colors indicate domain boundaries assigned by The Encyclopedia of Domains (TED) [40]. TED assignments for

A0A1S6KSF1 are shown in green (Domain 1; residues Ile2–His87), dark orange (Domain 2; Lys129–Ile271, Phe308–Ser372), and purple (Domain 3; Arg373–Leu496). Domain 1 of A0A1S6KSF9 (Ser2–Gln122) is shown in green. **(C)** Toxicity from expression of WP_025789713.1 alone or co-expressed with WP_025789712.1 in *E. coli* BL21-AI. Transformants harboring combinations of pPER5, pBAD33.1F, or the indicated expression plasmids were inoculated into LB supplemented with chloramphenicol, kanamycin (both for plasmid maintenance), and 0.4% [wt/vol] glucose (to repress expression). Cultures were incubated overnight at 37°C with constant shaking. The next day, cells were pelleted, washed twice with PBS, and normalized to an OD_{600} of 1.0. Serial 10-fold dilutions were spotted onto LB agar plates containing chloramphenicol, kanamycin, and either 0.4% [wt/vol] glucose (to maintain repression) or 0.025% [wt/vol] arabinose (to induce expression). Plates were incubated at 37°C for 24 hours and then inspected to assess growth.

To investigate the antibacterial functionality of WP_025789713.1, we inserted the corresponding CDS into pPER5, in-frame with a pelB leader sequence (for localization to the periplasm) and C-terminal myc-His tag, for expression in *E. coli* BL21-AI. Since pPER5 is a pBAD derivative, sequences cloned into the MCS of this vector are placed under the control of the *araBAD* promoter, allowing for arabinose-inducible, glucose-repressible expression. When plated on LB agar supplemented with arabinose, *E. coli* transformed with a WP_025789713.1 expression plasmid exhibited steep declines in viability as compared to those harboring an empty pPER5 control (**Fig 3C**). To evaluate WP_025789712.1 as an antidote to WP_025789713.1-mediated intoxication, WP_025789713.1 and WP_025789712.1 were then co-expressed from pPER5 and pBAD33.1F, respectively, resulting in a partial rescue of survival. Notably, high-level expression of immunity proteins for periplasmic effectors can prove toxic in itself [33]. For this reason, a low concentration (0.025% [wt/vol]) of arabinose was used in order to mitigate growth defects caused by overexpression of WP_025789712.1.

While these data provide evidence that WP_025789713.1 and WP_025789712.1 constitute a *bona fide* antibacterial effector toxin/immunity pair, additional work is needed to validate their association with and translocation by either T6S or a different system.

T6SS1 contributes to the lethality of *V. parahaemolyticus* 13-306/D4 against *L. vannamei* postlarvae under warm, marine-like conditions

We next sought to assess the indispensability of T6SS1 and T6SS2 within the context of shrimp infection by our representative VP_{AHPND} strain. To this end, we employed a small-scale challenge assay using the commercial shrimp species *L. vannamei* (whiteleg shrimp). Briefly, *L. vannamei* PL obtained from Miami Aquaculture were maintained in a filtered and aerated aquarium tank containing Artificial Seawater (ASW). Postlarvae (PL) between the age of PL24 and PL30 were allocated into foil-covered beakers filled with sterile ASW (3% salinity) and maintained at a temperature of 30°C, with aeration provided by sterile airstones. After a brief acclimation period, experiment beakers were inoculated with a phosphate-buffered saline (PBS) control or the indicated D4 strain at 1E6 CFU/mL, and mortality was assessed at 12, 24, and 48 hours post-infection (**Fig 4B** and **Dataset S4**).

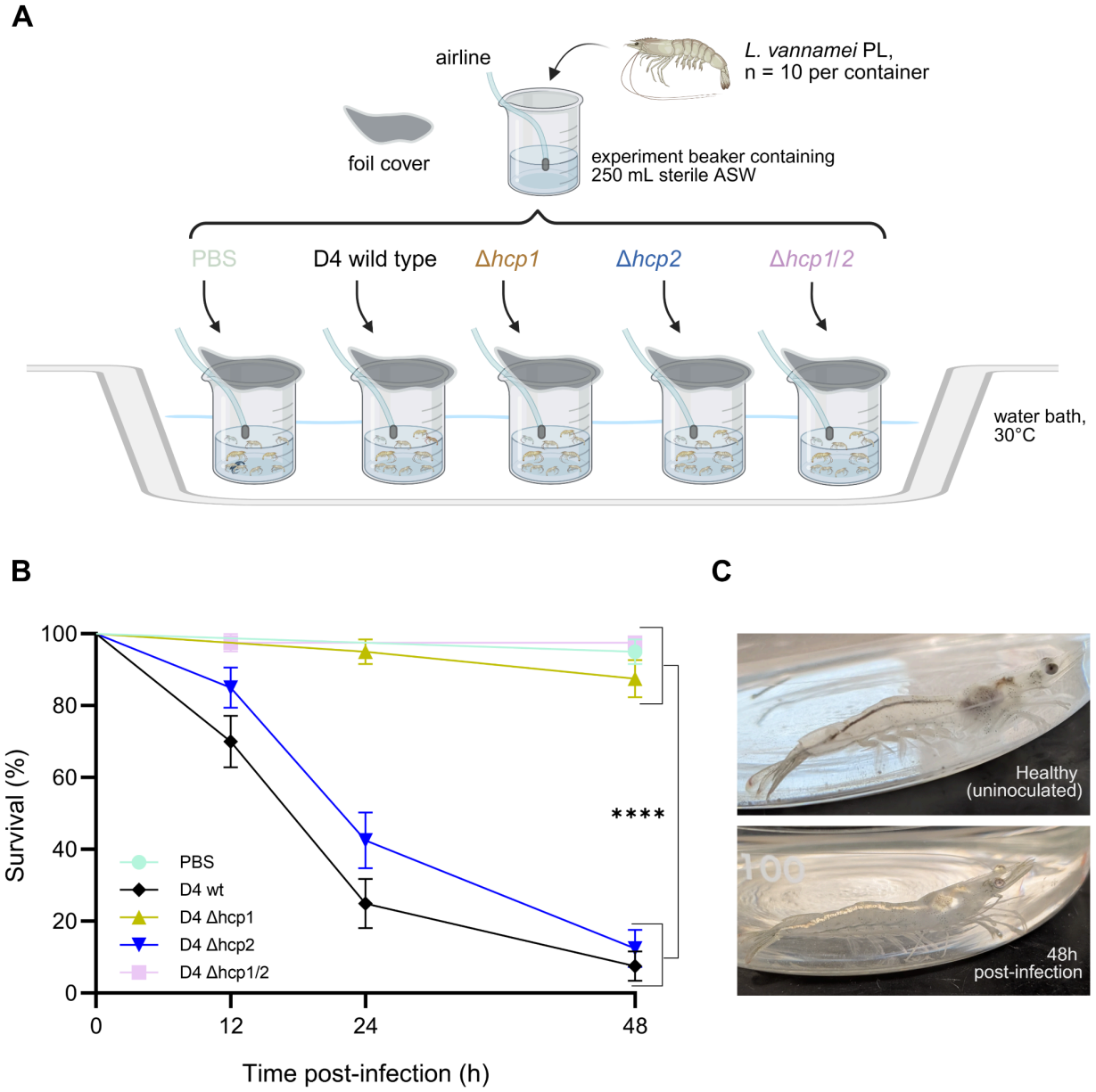

Fig 4. Immersion challenges of *L. vannamei* with D4 wild type and mutant strains. (A) Experimental setup for evaluating VP_{AHPND} virulence against *L. vannamei* postlarvae (PL). **(B)** Survival of *L. vannamei* PL following infection with *Vibrio parahaemolyticus* 13-306/D4 and derived mutants. Survival probabilities were plotted using Kaplan-Meier curves. Asterisks indicate curves with significant differences (Holm-adjusted $p < 0.0001$). Error bars represent 95% CI. **(C)** Representative images of an *L. Vannamei* PL before and after immersion challenge with the *V. parahaemolyticus* 13-306/D4 parent strain. The top panel depicts a healthy midgut with intact hepatopancreas. The bottom panel shows a moribund individual exhibiting characteristic signs of AHPND pathology, including discoloration and atrophy of the hepatopancreas.

Exposure of *L. vannamei* PL to the wild type strain of D4 resulted in mortality approaching 100% within 48 hours, consistent with previous reports for this isolate. Remarkably, both D4 Δ*hcp1* and D4

Δ*hcp1/2* were markedly attenuated in their ability to induce mortality in *L. vannamei* when compared to the wild type. Pairwise log-rank tests revealed significant differences in survival between most treatment groups (Holm-adjusted $p < 0.05$). Shrimp challenged with the wild type or Δ*hcp2* strains exhibited significantly reduced survival compared to Δ*hcp1*, Δ*hcp1/2*, or PBS controls ($p < 0.0001$), with no significant difference between Δ*hcp2* and the parent strain ($p = 0.32$). In contrast, survival curves for individuals challenged with Δ*hcp1*, Δ*hcp1/2*, and PBS were not significantly different from each other ($p > 0.3$), indicating that deletion of *hcp1* alone or in combination with *hcp2* strongly attenuates virulence. Dead or moribund PL challenged with wild type D4 or derivatives exhibited morphological and behavioral characteristics consistent with existing reports of AHPND pathology, namely discoloration and atrophy of the hepatopancreas (**Fig 4C**). Individuals that were putatively infected but still alive displayed lethargy punctuated by weak, “corkscrew” swimming.

To determine whether antagonism against host microbes is the primary contribution of T6S to virulence, we carried out an additional series of challenge experiments using *L. vannamei* with a depleted microbiome (**Figs 5A–B** and **Dataset S5**). In these trials, *L. vannamei* were treated with an antibiotic cocktail (see Materials and Methods for antibiotic cocktail formulation) for a 24 hour period, after which they were transferred to sterile ASW and infected as before. Bacterial titers from hepatopancreases of antibiotic-treated and untreated *L. vannamei* were estimated by plating serial 10-fold dilutions of homogenized midgut samples onto MLB agar and incubating at 30°C for 24 hours. Incubation of PL in antibiotic-treated ASW reduced the bacterial load of midgut samples to below our detection limit (approx. 2E3 CFU/g of tissue). In contrast, midguts from untreated individuals yielded approximately 1.4E6 ± 8.0E5 CFU/g (**Fig 5C** and **Dataset S5**).

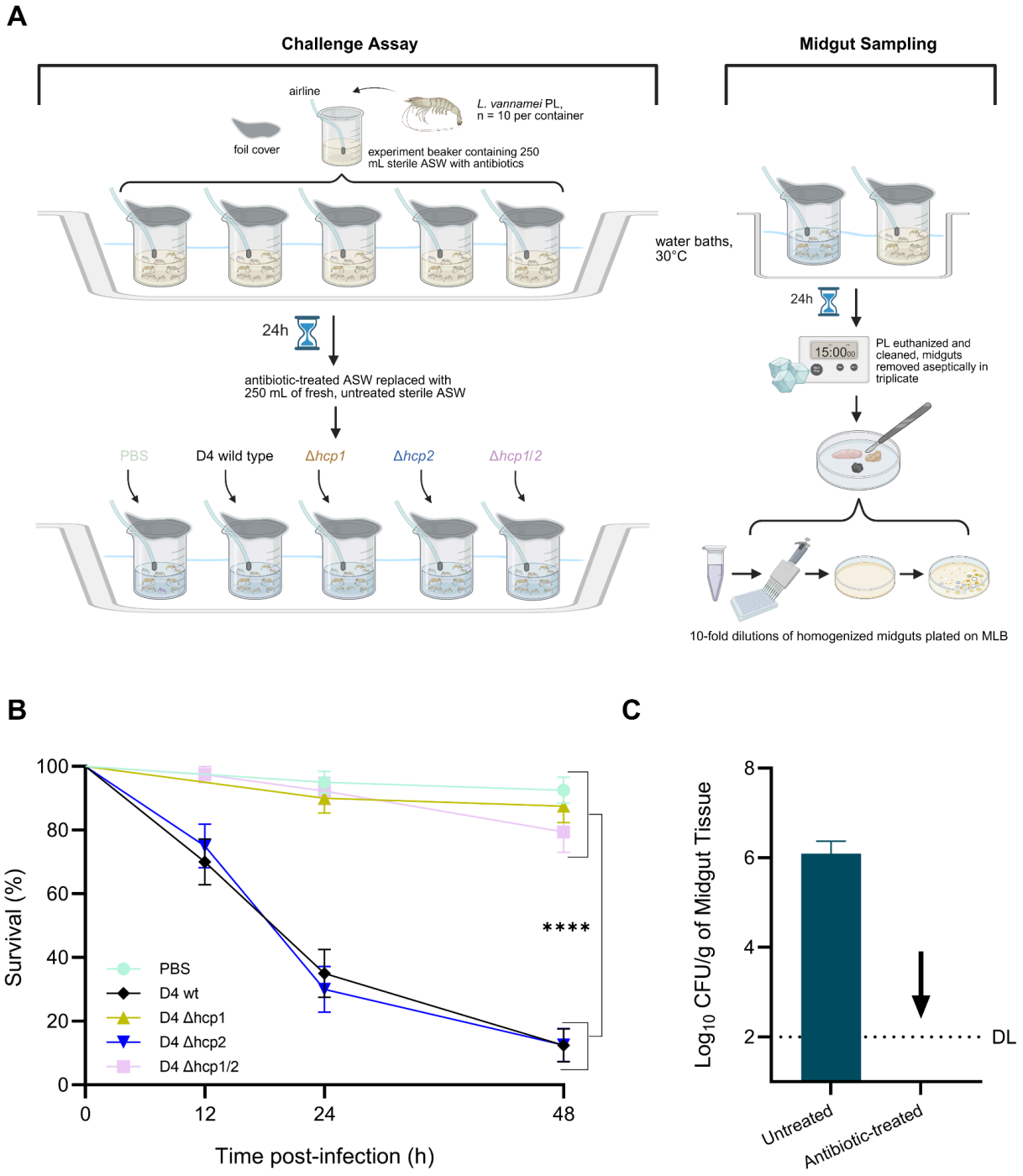

Fig 5. Immersion challenges of antibiotic-treated *L. vannamei* with D4 wild type and mutant strains. (A) Experiment setup for antibiotic pre-treatment, midgut sampling, and infection experiments against *L. vannamei* with a reduced microbiome. **(B)** Survival of antibiotic-treated *L. vannamei* following infection with *V. parahaemolyticus* strain 13-306/D4 and derived mutants. Survival probabilities were plotted using Kaplan-Meier curves. Asterisks indicate curves with significant differences (Holm-adjusted $p < 0.0001$). Error bars represent 95% CI. **(C)** Recovered culturable bacteria (Log_{10} CFU/g) in midgut

samples from antibiotic-treated or untreated *L. vannamei*. Dotted line represents the detection limit (DL). Error bars represent SEM. Down arrow represents values < detection limit.

Reduction of the *L. vannamei* microbiota via antibiotic administration did not eliminate discrepancies in the post-infection mortality caused by D4 Δ*hcp1* or Δ*hcp1/2* as compared with D4 Δ*hcp2* or the parent strain. Pairwise log-rank tests showed similar significant differences in survival to that of untreated PL. Shrimp challenged with the wild type or Δ*hcp2* strains exhibited significantly reduced survival compared to Δ*hcp1*, Δ*hcp1/2*, or PBS controls ($p < 0.0001$), with no significant difference between wild type and Δ*hcp2* ($p = 1$). Survival curves for Δ*hcp1*, Δ*hcp1/2*, and PBS were not significantly different from each other ($p > 0.41$) (**Dataset S5**).

Discussion

Mortality data from the *L. vannamei* challenge experiments indicate that the inability to utilize T6SS1 dramatically attenuates the lethality of D4 against *L. vannamei* PL under warm, high-salinity conditions. Contrastingly, T6SS2 does not appear to be critical to AHPND pathogenesis under these same conditions, despite our observation that T6SS1 and T6SS2 both mediate antibacterial activity *in vitro* under similar temperature and salinity conditions. We note that the water temperature and salinity conditions employed in this study were calibrated to reflect conditions that are applicable to *L. vannamei* aquaculture systems while also being conducive for T6SS1 activity in *V. parahaemolyticus* [6, 23, 41–43]. *L. vannamei* between PL24 and PL30 were used for infections to simulate the typical occurrence of AHPND outbreaks within 20–30 days after stocking of shrimp ponds [44, 45].

While the current study does not evidence T6SS2 as an important factor during shrimp infection, we speculate that modifying experimental parameters such as water temperature or salinity may influence the relative contributions of T6SS1 and T6SS2 to AHPND pathogenesis. For instance, T6SS2 may play a greater role in virulence under lower temperature and salinity conditions (e.g., 23–26°C and 1–2% salinity). We additionally propose that different VP_{AHPND} isolates, as well as related AHPND-causing Vibrios, may exhibit variation in the extent to which they employ T6S during infection.

Past hypotheses about the likely role of T6S in AHPND have focused on the ability of VP_{AHPND} to kill bacterial competitors within the host. To evaluate this model, we conducted additional challenge experiments using *L. vannamei* that had been pre-treated with an antibiotic cocktail to reduce naturally occurring bacterial loads. Unexpectedly, while estimated concentrations of bacteria in the midgut of treated PL were reduced, overall trends in post-infection mortality remained similar to prior experiments in this study. Currently, we are unable to provide strong evidence to support antagonism against host microbes as the sole mechanism by which T6SS1 contributes to mortality caused by VP_{AHPND}. However, this may be attributable to limitations of our study. Namely, while CFU/g of midgut samples from treated PL were reduced below our detection limit (approx. 2E3 CFU/g), this does not account for organisms in a VBNC state or otherwise unculturable taxa which may have survived the antibiotic cocktail. To our knowledge, a truly axenic *L. vannamei* system has not been developed. Therefore, future works that employ an axenic surrogate model (e.g., brine shrimp) may prove useful.

We suggest that the contribution of T6SS1 to VP_{AHPND} virulence, as reported here, could be multifactorial. For one, T6SS1 may play a direct role in colonization by mediating adhesion to host tissues. Yu et al. (2012) previously reported that T6SS1 contributes to the adhesion of *V. parahaemolyticus* to monolayers of Caco-2 intestinal epithelial cells [27]. However, as Caco-2 is a human cell line, further work is required to determine whether T6SS1 enhances attachment to the *L. vannamei* intestinal epithelium. Similarly, Pinkerton et al. (2019) demonstrated that downregulation of T6S, as achieved by A3009, interrupts the ability of VP_{AHPND} to associate with and invade the fish cell line CHSE-214 [29]. The same study further showed that A3009 attenuates *L. vannamei* mortality induced by

VP_{AHPND} [29]. Taken together, these data highlight the possibility that T6SS-dependent adhesion of *V. parahaemolyticus* to the *L. vannamei* intestine facilitates colonization and AHPND pathogenesis, and additional studies are warranted to evaluate this model.

A related possibility is that the large repetitive protein (WP_318301207.1) encoded at the end of the T6SS1 cluster fills a role comparable to the *A. fischeri* homolog TasL described by Speare et al. (2022), and could therefore facilitate aggregate formation or other collective behaviors [34]. While secretion of WP_318301207.1 by T6S is unlikely, inactivation of T6SS1 may somehow impact expression or localization of WP_318301207.1.

In a similar vein, perturbation of T6SS1 function might exert regulatory consequences that impact other virulence factors, namely the $PirA^{vp}$ and $PirB^{vp}$ toxins. Past studies have shown that deletion of T6SS core component genes can alter the non-T6SS secretome of Vibrios and other marine bacteria, with downstream effects on motility and adhesion [46–48]. Moreover, Bai et al. (2024) have recently described intracellular roles for the Hcp proteins of *Vibrio alginolyticus* as modulators of transport and metabolism [49]. Although any potential moonlighting functions of Hcp1 in *V. parahaemolyticus* remain to be explored, further experiments are necessary to elucidate whether disruption of T6SS1 may influence other pathogenicity determinants of VP_{AHPND}.

To conclude, the current study presents empirical evidence that T6SS1 serves as a determinant of VP_{AHPND} virulence against *L. vannamei* under warm, high-salinity conditions. While the underlying mechanism(s) involved await further investigation, we offer several possible explanations based on existing literature and genomic evidence. Lastly, this work identifies a novel plasmid-borne antibacterial effector/immunity pair that may contribute to interbacterial antagonism.

Materials and methods

Bacterial Strains and Media Used

The AHPND-causing *V. parahaemolyticus* strain 13-306/D4 (abbreviated D4) and *E. coli* strain S17-1 (λ-pir) were generous gifts from Kim Orth at the University of Texas Southwestern Medical Center and were used for various experiments reported here. *V. parahaemolyticus* strains were routinely grown at 30°C with continuous shaking (200 rpm) in marine Luria-Bertani (MLB) broth (LB adjusted to 3% [wt/vol] NaCl) or on marine minimal medium (MMM) agar plates (1.5% [wt/vol] agar, 2% [wt/vol] NaCl, 0.4% [wt/vol] galactose, 5 mM $MgSO_4$, 7 mM K_2SO_4, 77 mM K_2HPO_4, 35 mM KH_2PO_4, 2 mM NH_4Cl), supplemented with antibiotics when appropriate [6].

E. coli strain S17-1 (λ-pir) was used for maintenance and conjugation of pDM4 and derived plasmids. *E. coli* DH5α was used for cloning and plasmid maintenance, and as a prey strain for competition assays. Ectopic expression from arabinose-inducible vectors was carried out in *E. coli* BL21-AI. All *E. coli* strains were cultured at 37°C (30°C for competition assays) in LB broth or on LB agar plates, supplemented with chloramphenicol (20 µg/mL) or kanamycin (50 µg/mL) when necessary for plasmid maintenance. For a list of bacterial strains and plasmids used in this study, see **Supporting Information**.

Construction of in-frame deletion mutants

Mutants of *V. parahaemolyticus* harboring in-frame deletions of target genes were generated via allelic exchange using the CmR OriR6K suicide plasmid pDM4 as previously reported [6]. In brief, 1-kb regions directly upstream and downstream of the target gene were amplified from a genomic DNA template and inserted via Gibson Assembly into a pDM4 plasmid linearized with SacI-HF. The resulting

constructs were first transformed into *E. coli* S17-1 (λ-pir) and then subsequently conjugated into *V. parahaemolyticus*. Transconjugants were selected for using MMM containing 10 µg/mL chloramphenicol and were additionally screened for sucrose sensitivity. Transconjugants were streaked onto MMM without chloramphenicol for outgrowth, and then subsequently transferred to MMM supplemented with sucrose for counterselection. Putative secondary recombinants were checked for chloramphenicol sensitivity, and PCR screens were carried out to identify and confirm allelic exchange mutants harboring the intended deletions. For a list of primers used in this study, see **Supporting Information**.

Bacterial competition assays

T6SS competition assays were performed as described previously, with minor modifications [6]. Briefly, cultures of attacker and prey strains were grown overnight in MLB (*V. parahaemolyticus*) or LB (*E. coli*). Overnight cultures grown for 16 hours were pelleted, washed twice with phosphate-buffered saline (PBS), and normalized to an optical density at 600 nm (OD_{600}) of 0.5 before being mixed at a 4:1 ratio (attacker-to-prey) and spotted (25 µL) in triplicate onto 12-well MLB agar plates. Competition plates were incubated for 4 hours at 30°C. Prey CFU/mL at the start of the assay (T0) was determined by spotting 10-fold serial dilutions of mixed cells onto LB plates containing 20 µg/mL chloramphenicol for selection of *E. coli* prey harboring an empty pBAD33.1 plasmid. At the end of the assay (T4), competition spots were harvested, and surviving prey CFU/mL was determined by spotting 10-fold serial dilutions as above (**Dataset S1**). Assays were repeated twice with similar results.

L. vannamei maintenance

Disease-free *L. vannamei* postlarvae (PL) derived from a Specific-Pathogen-Free (SPF) broodstock were supplied by Miami Aquaculture (Boynton Beach, Florida, USA), and maintained in an aquarium tank filled with approximately 25 L of Artificial Seawater (ASW; 30 grams Instant Ocean® per liter of deionized water) with filtration (Tetra Whisper EX30 Power Filter) and aeration with attached airstones. Maintenance tank water was kept at a temperature of 30 ± 1°C using an Ultra-Slim Submersible Aquarium Heater (Fluval, Montreal, Canada). Tank water was maintained at a pH of 7.2–7.6 and salinity of 3%. Lighting was provided on a 12 hour schedule, and tank water was refreshed on a biweekly basis. PL were fed approximately 10% body weight per day of PL Raceway Plus feed (Zeigler, Gardners, PA).

L. vannamei infections

L. vannamei ranging from PL24 to PL30 (average weight 0.244 ± 0.07 g) were transferred to foil-covered experiment beakers filled with 250 mL sterile ASW and maintained under conditions similar to the holding tank (i.e., water temperature of 30°C, 3% salinity, with aeration provided by sterile airstones and lighting on a 12 hour cycle). Ten PL were transferred to each beaker, after which time they were monitored for signs of stress or erratic behavior prior to the start of the challenge. PL were then inoculated with the appropriate *V. parahaemolyticus* 13-306/D4 strain (see Inocula Preparation) or a PBS control.

During the challenge, PL were fed approximately 10% of their estimated body weight once per day, calculated based on the number of live PL at feeding time. Mortality of PL was determined at 12, 24, and 48 hours post-infection (**Dataset S4**). Live/dead determinations were made on the basis of morphological observations and movement or lack thereof. PL that displayed signs of atrophy and did not move for 5 minutes during observation were defined as non-viable. Any missing PL were assumed dead (*L. vannamei* are scavengers and will cannibalize the remains of dead individuals).

For infections using antibiotic-treated *L. vannamei*, PL were first sorted into experiment beakers containing 250 mL sterile, antibiotic-treated ASW (see Antibiotic Cocktail Formulation). Following a 24 hour incubation at 30°C, antibiotic-treated ASW was replaced with sterile, untreated ASW. After a brief acclimation period, PL were inoculated as above, and mortality data were collected at 12, 24, and 48 hours post-infection (**Dataset S5**). All infection experiments were carried out in duplicate.

Kaplan-Meier survival curves were generated using Prism, and statistical differences between groups were determined by log-rank (Mantel-Cox) test. Multiple pairwise comparisons were performed in R (v4.3.2) using the pairwise_survdiff() function in the survminer package with Holm correction for multiple testing.

Antibiotic cocktail formulation

An antibiotic composition was identified that would be well-tolerated by *L. vannamei* PL and effective in reducing CFU recovered from the midguts of treated individuals. The antibiotic resistance profile of the D4 isolate was also considered to minimize the potential impact of leftover drug residues in *L. vannamei* tissues on Vp_{AHPND} pathogenesis. A solution consisting of sterile ASW freshly supplemented with colistin (10 µg/mL), tetracycline (10 µg/mL), ampicillin (100 µg/mL), chloramphenicol (10 µg/mL), vancomycin (50 µg/mL), and kanamycin (50 µg/mL) best met the above criteria, and was employed in subsequent experiments. Although D4 lacks chloramphenicol resistance, exposure to the cocktail did not show an effect of residual antibiotics on post-infection mortality, and the rapid elimination of chloramphenicol from *L. vannamei* tissues has been previously reported [50].

Inocula preparation

Inocula were prepared as follows. Colonies of D4 wild type and mutant strains were picked from MMM agar plates, inoculated into MLB, and grown overnight at 30°C with continuous shaking (200 rpm). The following day, cells were pelleted, washed twice with PBS, and normalized to an OD_{600} of 0.5. Experiment beakers stocked with *L. vannamei* PL in 250 mL of ASW were then inoculated with PBS (negative control) or an appropriate volume of the designated D4 strain to obtain a final inoculum density of approximately 1E6 CFU/mL. The actual CFU/mL of each inoculum was determined by plating serial 10-fold dilutions on Thiosulfate–citrate–bile salts–sucrose (TCBS) agar or MMM agar plates.

Midgut sample collection

Experiment beakers containing *L. vannamei* in sterile, antibiotic-treated or untreated ASW were prepared as above and incubated at 30°C for 24 hours with aeration provided by an aquarium pump and sterile airstones. Midgut samples (hepatopancreas and intestines) were collected following a modified procedure based on Soto-Rodriguez et al. (2015) [51]. Briefly, *L. vannamei* were euthanized by placing their beakers on ice, then rinsed first with 70% ethanol, and then sterile ASW. Midguts were aseptically dissected using a sterile blade and placed into microcentrifuge tubes for weighing, then homogenized individually in 100 µL of sterile ASW for every 10 mg of tissue. Serial 10-fold dilutions of the resulting homogenates were made in sterile ASW and plated on MLB agar. Plates were incubated at 30°C for 24 hours and then inspected for CFU determinations. All samples were prepared in triplicate.

Growth experiments

Growth curve experiments were carried out on a plate reader as previously described, with modifications [52]. Briefly, starter cultures of *V. parahaemolyticus* wild type and mutant strains were grown in MLB overnight at 30°C with continuous shaking (200 rpm). The following day, cultures were washed with PBS and normalized to an OD_{600} of 0.1 in fresh MLB, then aliquoted in quadruplicate (200 µL per well) into a 96-well plate. Plates were incubated in a BioTek Cytation 5 microplate reader (Agilent, Santa Clara, CA) at 30°C with continuous shaking. Growth was measured as OD_{600} every hour over the course of 8 hours. Experiments were repeated twice with similar results (**Dataset S2**).

Sequence analysis and effector prediction

A complete genome assembly for *Vibrio parahaemolyticus* 13-306/D4 has been submitted to the NCBI GenBank database (Submission ID: SUB15344673) and is a revised version of the draft assembly initially deposited under accessions CP180435–CP180437. New accession numbers reflecting the updated assembly will be provided once assigned.

The NCBI BLAST suite was employed to survey the *V. parahaemolyticus* 13-306/D4 genome for homologs of previously reported effectors. An amino acid FASTA file for the D4 genome was obtained from The Rapid Annotations using Subsystems Technology (RAST) server and used as a query against a curated list of T6SS effector proteins from the literature [53, 54]. Protein accession and locus information for predicted effectors was gathered from the NCBI database and is summarized in **Table 1** and **Dataset S3**. Structure prediction and other analyses of WP_025789713.1 and WP_025789712.1 were carried out using the MPI Bioinformatics Toolkit [55]. Models AF-A0A1S6KSF1-F1-v4 (WP_025789713.1) and AF-A0A1S6KSF9-F1-v4 (WP_025789712.1) were retrieved from the AlphaFold Protein Structure Database (https://alphafold.ebi.ac.uk/) [39]. Default parameters were used for all software unless otherwise noted.

Plasmid construction for ectopic expression

For arabinose-inducible, glucose-repressible expression of WP_025789713.1, the corresponding CDS was amplified from *V. parahaemolyticus* 13-306/D4 and inserted into pPER5 in-frame with a pelB leader sequence and a C-terminal myc-His tag. The CDS of WP_025789712.1 was likewise amplified and inserted into pBAD33.1F in-frame with a C-terminal FLAG tag sequence. All expression plasmids were generated by means of Gibson Assembly using compatible primers. For a list of primer sequences and plasmids employed in this study, see **Supporting Information**.

Bacterial intoxication assays

To assess toxicity resulting from expression of WP_025789713.1, either alone or co-expressed with WP_025789712.1, *E. coli* BL21-AI were co-transformed with combinations of pPER5_WP_025789713.1, pBAD33.1F_WP_025789712.1, or the respective empty vector controls. Fresh co-transformants were inoculated into LB supplemented with 0.4% [wt/vol] glucose, 50 µg/mL kanamycin, and 20 µg/mL chloramphenicol and grown overnight at 37°C with constant shaking. The following day, cultures were washed twice and normalized to an OD_{600} of 1.0 in sterile PBS. Serial 10-fold dilutions were then spotted onto LB agar containing 50 µg/mL kanamycin, 20 µg/mL chloramphenicol, and either 0.4% [wt/vol] glucose or 0.025% [wt/vol] arabinose for repression or induction of expression, respectively. Plates were inspected visually after a 24 hour incubation at 37°C.

References

1. Lee C-T, Chen IT, Yang Y-T, Ko T-P, Huang Y-T, Huang J-Y, et al. The opportunistic marine pathogen *Vibrio parahaemolyticus* becomes virulent by acquiring a plasmid that expresses a deadly toxin. Proc Natl Acad Sci U S A. 2015;112(34):10798-803.
2. Tang K, Bondad-Reantaso M. Impacts of acute hepatopancreatic necrosis disease on commercial shrimp aquaculture. Rev Sci Tech. 2019;38:477-90.
3. Yan Y, Lu H, Liang X, Xu T, Yan S, Yu Y, Wang Y. The virulence plasmid associated with AHPND in shrimp appears to have originated from *Vibrio owensii* through a process of homologous recombination of parental plasmids and the transposable insertion of two large fragments. J Invertebr Pathol. 2024 Sep 1;206:108173.
4. Kumar V, Roy S, Behera BK, Bossier P, Das BK. Acute hepatopancreatic necrosis disease (AHPND): Virulence, pathogenesis and mitigation strategies in shrimp aquaculture. Toxins (Basel). 2021;13(8):524.
5. Castellanos A, Restrepo L, Bajaña L, Betancourt I, Bayot B, Reyes A. Genomic and evolutionary features of nine AHPND positive *Vibrio parahaemolyticus* strains isolated from South American shrimp farms. Microbiol Spectr. 2023;11(4):e04851-22.
6. Li P, Kinch LN, Ray A, Dalia AB, Cong Q, Nunan LM, et al. Acute hepatopancreatic necrosis disease-causing *Vibrio parahaemolyticus* strains maintain an antibacterial type VI secretion system with versatile effector repertoires. Appl Environ Microbiol. 2017;83(13):AEM.00737-17.
7. Wang R, Xiao J, Wang Q, Zhao W, Liu X, Liu Y, et al. Genomic analysis of a new type VI secretion system in *Vibrio parahaemolyticus* and its implications for environmental adaptation in shrimp ponds. Can J Microbiol. 2022;69(1):53-61.
8. Pukatzki S, Ma AT, Sturtevant D, Krastins B, Sarracino D, Nelson WC, et al. Identification of a conserved bacterial protein secretion system in *Vibrio cholerae* using the *Dictyostelium* host model system. Proc Natl Acad Sci U S A. 2006;103(5):1528-33.
9. Russell AB, Peterson SB, Mougous JD. Type VI secretion system effectors: Poisons with a purpose. Nat Rev Microbiol. 2014;12(2):137-48.
10. Zoued A, Brunet YR, Durand E, Aschtgen M-S, Logger L, Douzi B, et al. Architecture and assembly of the Type VI secretion system. Biochim Biophys Acta Mol Cell Res. 2014;1843(8):1664-73.
11. Bernard CS, Brunet YR, Gueguen E, Cascales E. Nooks and crannies in type VI secretion regulation. J Bacteriol. 2010;192(15):3850-60.
12. Wettstadt S. Should I kill or should I go: T6SS regulation networks in *Vibrio*. Environ Microbiol. 2020;22(1):1-4.
13. Hernandez RE, Gallegos-Monterrosa R, Coulthurst SJ. Type VI secretion system effector proteins: Effective weapons for bacterial competitiveness. Cell Microbiol. 2020;22(9):e13222.
14. Jurėnas D, Journet L. Activity, delivery, and diversity of type VI secretion effectors. Mol Microbiol. 2021;115(3):383-94.
15. Sana TG, Berni B, Bleves S. The T6SSs of *Pseudomonas aeruginosa* Strain PAO1 and their effectors: Beyond bacterial-cell targeting. Front Cell Infect Microbiol. 2016;6:112.
16. Jana B, Fridman CM, Bosis E, Salomon D. A modular effector with a DNase domain and a marker for T6SS substrates. Nat Commun. 2019;10(1):4725.

17. Wood TE, Howard SA, Förster A, Nolan LM, Manoli E, Bullen NP, et al. The *Pseudomonas aeruginosa* T6SS delivers a periplasmic toxin that disrupts bacterial cell morphology. Cell Rep. 2019;29(1):187-201.e7.
18. Ahmad S, Wang B, Walker MD, Tran H-KR, Stogios PJ, Savchenko A, et al. An interbacterial toxin inhibits target cell growth by synthesizing (p)ppApp. Nature. 2019;575(7784):674-8.
19. Yang X, Pan J, Wang Y, Shen X. Type VI secretion systems present new insights on pathogenic *Yersinia*. Front Cell Infect Microbiol. 2018;8:195.
20. Church SR, Lux T, Baker-Austin C, Buddington SP, Michell SL. *Vibrio vulnificus* type 6 secretion system 1 contains anti-bacterial properties. PLoS One. 2016;11(10):e0165500.
21. Cohen H, Fridman CM, Gerlic M, Salomon D. A *Vibrio* T6SS-mediated lethality in an aquatic animal model. Microbiol Spectr. 2023;11(4):e01093-23.
22. Hachani A, Wood TE, Filloux A. Type VI secretion and anti-host effectors. Curr Opin Microbiol. 2016;29:81-93.
23. Salomon D, Gonzalez H, Updegraff BL, Orth K. *Vibrio parahaemolyticus* type VI secretion system 1 is activated in marine conditions to target bacteria, and is differentially regulated from system 2. PLoS One. 2013;8(4):e61086.
24. Ben-Yaakov R, Salomon D. The regulatory network of *Vibrio parahaemolyticus* type VI secretion system 1. Environ Microbiol. 2019;21(7):2248-60.
25. Tchelet D, Keppel K, Bosis E, Salomon D. *Vibrio parahaemolyticus* T6SS2 effector repertoires. Gut Microbes. 2023;15(1):2216669.
26. Metzger LC, Matthey N, Stoudmann C, Collas EJ, Blokesch M. Ecological implications of gene regulation by TfoX and TfoY among diverse *Vibrio* species. Environ Microbiol. 2019;21(7):2231-47.
27. Yu Y, Yang H, Li J, Zhang P, Wu B, Zhu B, et al. Putative type VI secretion systems of *Vibrio parahaemolyticus* contribute to adhesion to cultured cell monolayers. Arch Microbiol. 2012;194:827-35.
28. Zhang L, Osei-Adjei G, Zhang Y, Gao H, Yang W, Zhou D, et al. CalR is required for the expression of T6SS2 and the adhesion of *Vibrio parahaemolyticus* to HeLa cells. Arch Microbiol. 2017;199:931-8.
29. Pinkerton L, Linton M, Kelly C, Ward P, Gradisteanu Pircalabioru G, Pet I, Stef L, Sima F, Adamov T, Gundogdu O, Corcionivoschi N. Attenuation of *Vibrio parahaemolyticus* virulence factors by a mixture of natural antimicrobials. Microorganisms. 2019 Dec 11;7(12):679.
30. Nunan L, Lightner D, Pantoja C, Gomez-Jimenez S. Detection of acute hepatopancreatic necrosis disease (AHPND) in Mexico. Dis Aquat Organ. 2014;111(1):81-6.
31. Harrison KJ, Crécy-Lagard VD, Zallot R. Gene graphics: A genomic neighborhood data visualization web application. Bioinformatics. 2018 Apr 15;34(8):1406-8.
32. Salomon D, Kinch LN, Trudgian DC, Guo X, Klimko JA, Grishin NV, et al. Marker for type VI secretion system effectors. Proc Natl Acad Sci U S A. 2014;111(25):9271-6.
33. Dar Y, Jana B, Bosis E, Salomon D. A binary effector module secreted by a type VI secretion system. EMBO Rep. 2022;23(1):e53981.
34. Speare L, Woo M, Dunn AK, Septer AN. A putative lipoprotein mediates cell-cell contact for type VI secretion system-dependent killing of specific competitors. MBio. 2022 Apr 26;13(2):e03085-21.
35. LaPorte JP, Spinard EJ, Cavanagh D, Gomez-Chiarri M, Rowley DC, Mekalanos JJ, Mittraparp-Arthorn P, Nelson DR. Draft genome sequence of *Vibrio parahaemolyticus* PSU5579, isolated during an outbreak of acute hepatopancreatic necrosis disease in Thailand. Microbiol Resour Announc. 2023 Feb 16;12(2):e00873-22.

36. Mass S, Cohen H, Podicheti R, Rusch DB, Gerlic M, Ushijima B, van Kessel JC, Bosis E, Salomon D. The coral pathogen *Vibrio coralliilyticus* uses a T6SS to secrete a group of novel anti-eukaryotic effectors that contribute to virulence. PLoS Biol. 2024 Sep 3;22(9):e3002734.
37. De Maayer P, Venter SN, Kamber T, Duffy B, Coutinho TA, Smits TH. Comparative genomics of the type VI secretion systems of *Pantoea* and *Erwinia* species reveals the presence of putative effector islands that may be translocated by the VgrG and Hcp proteins. BMC Genomics. 2011 Dec;12:1-5.
38. Kanarek K, Fridman CM, Bosis E, Salomon D. The RIX domain defines a class of polymorphic T6SS effectors and secreted adaptors. Nat Commun. 2023 Aug 17;14(1):4983.
39. Jumper J, Evans R, Pritzel A, Green T, Figurnov M, Ronneberger O, Tunyasuvunakool K, Bates R, Žídek A, Potapenko A, Bridgland A. Highly accurate protein structure prediction with AlphaFold. Nature. 2021 Aug;596(7873):583-9.
40. Lau AM, Bordin N, Kandathil SM, Sillitoe I, Waman VP, Wells J, Orengo CA, Jones DT. Exploring structural diversity across the protein universe with the Encyclopedia of Domains. Science. 2024 Nov 1;386(6721):eadq4946.
41. Abdelrahman HA, Abebe A, Boyd CE. Influence of variation in water temperature on survival, growth and yield of Pacific white shrimp *Litopenaeus vannamei* in inland ponds for low-salinity culture. Aquac Res. 2019;50(2):658-72.
42. Lester LJ, Pante MR. Penaeid temperature and salinity responses. Dev Aquac Fish Sci. 1992;23:515-34.
43. Wickins JF, Lee DOC. Crustacean farming: ranching and culture: John Wiley & Sons; 2008. (This is a book, so the format differs slightly. This looks correct for a book.)
44. De Schryver P, Defoirdt T, Sorgeloos P. Early mortality syndrome outbreaks: A microbial management issue in shrimp farming? PLoS Pathog. 2014;10(4):e1003919.
45. Lai H-C, Ng TH, Ando M, Lee C-T, Chen I-T, Chuang J-C, et al. Pathogenesis of acute hepatopancreatic necrosis disease (AHPND) in shrimp. Fish Shellfish Immunol. 2015;47(2):1006-14.
46. Wang YD, Gong JS, Guan YC, Zhao ZL, Cai YN, Shan XF. Hcp1 regulates flagella of *Aeromonas veronii* TH0426 to reduce virulence. Aquaculture. 2023 Nov 15;576:739899.
47. Liu L, Hao S, Lan R, Wang G, Xiao D, Sun H, Xu J. The type VI secretion system modulates flagellar gene expression and secretion in *Citrobacter freundii* and contributes to adhesion and cytotoxicity to host cells. Infect Immun. 2015 Jul;83(7):2596-604.
48. Wu S, Tang J, Wang B, Cai J, Jian J. Roles of Hcp2, a hallmark of T6SS2 in motility, adhesive capacity, and pathogenicity of *Vibrio alginolyticus*. Microorganisms. 2023 Nov 30;11(12):2893.
49. Bai XR, Liu PX, Wang WC, Jin YH, Wang Q, Qi Y, Zhang XY, Sun WD, Fang WH, Han XG, Jiang W. TssL2 of T6SS2 is required for mobility, biofilm formation, wrinkly phenotype formation, and virulence of *Vibrio parahaemolyticus* SH112. Appl Microbiol Biotechnol. 2024 Dec;108(1):1-21.
50. Suseno H, Hudiyono S, Muslim M. Elimination of chloramphenicol by tiger shrimp (*Penaeus monodon*) and white shrimp (*Litopenaeus vannamei*). HAYATI J Biosci. 2016 Jul 1;23(3):117-20.
51. Soto-Rodriguez SA, Gomez-Gil B, Lozano-Olvera R, Betancourt-Lozano M, Morales-Covarrubias MS. Field and experimental evidence of *Vibrio parahaemolyticus* as the causative agent of acute hepatopancreatic necrosis disease of cultured shrimp (*Litopenaeus vannamei*) in Northwestern Mexico. Appl Environ Microbiol. 2015 Mar 1;81(5):1689-99.
52. Chimalapati S, Lafrance AE, Chen L, Orth K. *Vibrio parahaemolyticus*: Basic techniques for growth, genetic manipulation, and analysis of virulence factors. Curr Protoc Microbiol. 2020 Dec;59(1):e131.
53. Aziz RK, Bartels D, Best AA, DeJongh M, Disz T, Edwards RA, et al. The RAST server: Rapid annotations using subsystems technology. BMC Genomics. 2008;9:1-15.

54. Altschul SF, Gish W, Miller W, Myers EW, Lipman DJ. Basic local alignment search tool. J Mol Biol. 1990;215(3):403-10.
55. Gabler F, Nam SZ, Till S, Mirdita M, Steinegger M, Söding J, Lupas AN, Alva V. Protein sequence analysis using the MPI bioinformatics toolkit. Curr Protoc Bioinformatics. 2020 Dec;72(1):e108.